Electronic Supplementary Material (ESI) for Journal of Materials Chemistry A.

Hybrid mesoporous aluminosilicate catalysts obtained by non-hydrolytic sol-gel for ethanol dehydration

Ales Styskalik,[a,b] Imene Kordoghli,[a] Claude Poleunis,[a] Arnaud Delcorte,[a] Zdenek Moravec,[b] Lucie Simonikova,[b] Viktor Kanicky,[b] Carmela Aprile,[c] Luca Fusaro,[c] Damien P. Debecker*[a]

[a]Institute of Condensed Matter and Nanoscience (IMCN), UCLouvain, Place Louis Pasteur 1, 1348 Louvain-La-Neuve, Belgium

[b]Masaryk University, Department of Chemistry, Kotlarska 2, CZ-61137 Brno, Czech Republic

[c]Department of Chemistry, Unit of Nanomaterials Chemistry, University of Namur, 5000 Namur, Belgium

*Corresponding author (damien.debecker@uclouvain.be).

Spectroscopic characterization data.

15Si-1MeSi-1Al: IR (KBr, cm^{-1}) ν : 585 w (ρ Si−O−Si), 806 m (ν_s Si−O−Si), 946 vw (ν Si−OH), 1014 vs, 1048 vs (ν Si−O−Si/Al), 1213 shoulder, 1281 vw (δ_s $SiCH_3$), 1623 w (δ OH), 2979 w (ν_{as} CH_3), 3300 m-broad (ν OH).

^{29}Si MAS NMR (ppm) δ : −56 (broad, $CH_3Si(OSi)(OH)_2$ + $CH_3Si(OSi)_2(OH)$), −101 (broad, $Si(OSi)_2(OH/OAl)_2$) + $Si(OSi)_3(OH/OAl)$ + $Si(OSi)_4$).

^{27}Al MAS NMR (ppm) δ : 0 (AlO_6), 28 (shoulder, AlO_5), 53 (AlO_4).

15Si-1MeSi-0.25Al: IR (KBr, cm^{-1}) ν : 436 vs, 568 w (ρ Si−O−Si), 802 m (ν_s Si−O−Si), 951 m (ν Si−OH), 1058 vs (ν Si−O−Si/Al), 1178 shoulder, 1282 vw (δ_s $SiCH_3$), 1624 w (δ OH), 2979 vw (ν_{as} CH_3), 3300 m-broad (ν OH).

^{29}Si CPMAS NMR (ppm) δ : −58 ($CH_3Si(OSi)(OH)_2$), −66 ($CH_3Si(OSi)_2(OH)$), −95 ($Si(OSi)_2(OH/OAl)_2$), −103 ($Si(OSi)_3(OH/OAl)$), −112 ($Si(OSi)_4$).

^{27}Al MAS NMR (ppm) δ : 0 (AlO_6), 53 (AlO_4).

15Si-1MeSi-0.5Al: IR (KBr, cm^{-1}) ν : 442 vs, 570 w (ρ Si−O−Si), 798 m (ν_s Si−O−Si), 957 m (ν Si−OH), 1060 vs (ν Si−O−Si/Al), 1201 shoulder, 1280 vw (δ_s $SiCH_3$), 1626 w (δ OH), 3300 m-broad (ν OH).

^{29}Si CPMAS NMR (ppm) δ : −54 ($CH_3Si(OSi)(OH)_2$), −62 ($CH_3Si(OSi)_2(OH)$), −94 ($Si(OSi)_2(OH/OAl)_2$), −102 ($Si(OSi)_3(OH/OAl)$), −113 ($Si(OSi)_4$).

^{27}Al MAS NMR (ppm) δ : 0 (AlO_6), 52 (AlO_4).

15Si-1MeSi-2Al: IR (KBr, cm^{-1}) ν : 442 vs, 576 w (ρ Si−O−Si), 798 m (ν_s Si−O−Si), 929 w (ν Si−OH), 1056 vs (ν Si−O−Si/Al), 1203 shoulder, 1278 vw (δ_s $SiCH_3$), 1628 w (δ OH), 3300 m-broad (ν OH).

^{29}Si CPMAS NMR (ppm) δ : −53 ($CH_3Si(OSi)(OH)_2$), −63 ($CH_3Si(OSi)_2(OH)$), −92 ($Si(OSi)_2(OH/OAl)_2$), −101 ($Si(OSi)_3(OH/OAl)$), −112 ($Si(OSi)_4$).

^{27}Al MAS NMR (ppm) δ : 0 (AlO_6), 29 (shoulder, AlO_5), 53 (AlO_4).

16Si-1Al: IR (KBr, cm^{-1}) ν : 592 w (ρ Si−O−Si), 804 m (ν_s Si−O−Si), 946 m (ν Si−OH), 1058 vs (ν Si−O−Si/Al), 1198 shoulder, 1631 w (δ OH), 3300 m-broad (ν OH).

^{29}Si CPMAS NMR (ppm) δ : −92 ($Si(OSi)_2(OH/OAl)_2$), −102 ($Si(OSi)_3(OH/OAl)$), −112 ($Si(OSi)_4$).

^{27}Al MAS NMR (ppm) δ : 0 (AlO_6), 28 (shoulder, AlO_5), 53 (AlO_4).

15Si-1MeSi-1DAl: IR (KBr, cm^{-1}) ν : 438 vs, 576 w (ρ Si−O−Si), 800 m (ν_s Si−O−Si), 951 m (ν Si−OH), 1056 vs (ν Si−O−Si/Al), 1204 shoulder, 1278 vw (δ_s $SiCH_3$), 1629 w (δ OH), 3300 m-broad (ν OH).

^{29}Si CPMAS NMR (ppm) δ : −63 ($CH_3Si(OSi)_2(OH)$), −92 ($Si(OSi)_2(OH/OAl)_2$), −101 ($Si(OSi)_3(OH/OAl)$), −111 ($Si(OSi)_4$).

^{27}Al MAS NMR (ppm) δ : 0 (AlO_6), 26 (shoulder, AlO_5), 53 (AlO_4).

14Si-2MeSi-1Al: IR (KBr, cm^{-1}) ν : 592 w (ρ Si−O−Si), 802 m (ν_s Si−O−Si), 950 w (ν Si−OH), 1051 vs (ν Si−O−Si/Al), 1197 shoulder, 1281 w (δ_s $SiCH_3$), 1627 w (δ OH), 2981 w (ν_{as} CH_3), 3300 m-broad (ν OH).

^{29}Si MAS NMR (ppm) δ : −60 (broad, $CH_3Si(OSi)(OH)_2$ + $CH_3Si(OSi)_2(OH)$), −107 (broad, $Si(OSi)_2(OH/OAl)_2$) + $Si(OSi)_3(OH/OAl)$ + $Si(OSi)_4$).

^{27}Al MAS NMR (ppm) δ : 0 (AlO_6), 27 (AlO_5), 53 (AlO_4).

13Si-3MeSi-1Al: IR (KBr, cm^{-1}) ν : 442 m, 589 w (ρ Si−O−Si), 800 m (ν_s Si−O−Si), 833 shoulder (ρ_{as} $SiCH_3$), 934 vw (ν Si−OH), 1047 vs (ν Si−O−Si/Al), 1200 shoulder, 1280 w (δ_s $SiCH_3$), 1628 w (δ OH), 2981 vw (ν_{as} CH_3), 3300 m-broad (ν OH).

^{29}Si MAS NMR (ppm) δ : −64 (broad, $CH_3Si(OSi)(OH)_2$ + $CH_3Si(OSi)_2(OH)$), −109 (broad, $Si(OSi)_2(OH/OAl)_2$) + $Si(OSi)_3(OH/OAl)$ + $Si(OSi)_4$).

^{27}Al MAS NMR (ppm) δ : 0 (AlO_6), 27 (shoulder, AlO_5), 52 (AlO_4).

Table 1S: Synthesis (amount of precursors introduced in the preparation) and characterization of hybrid aluminosilicate catalysts in terms of bulk (ICP-OES) and surface (XPS) composition.

Sample	n_{Si} (mmol)	n_{RSi} (mmol)	n_{Al} (mmol)	n_{DIPE} (mmol)	Si:Al ratio Theor[a]/ICP/XPS (-)
15Si-1MeSi-1Al	26.87	1.779	1.822	59.89	15.7/16.3/24.2
15Si-1MeSi-0.25Al	26.77	1.865	0.463	59.03	61.8/69.3/72.6
15Si-1MeSi-0.5Al	26.82	1.798	0.903	57.66	31.7/33.2/33.5
15Si-1MeSi-2Al	26.80	1.792	3.553	61.71	8.0/6.8/15.0
14Si-2MeSi-1Al	25.04	3.539	1.843	58.00	15.5/17.2/27.8
13Si-3MeSi-1Al	23.49	5.332	1.827	57.16	15.8/14.1/24.5
16Si-1Al	28.63	-	1.762	60.09	16.2/17.5/30.0
15Si-1MeSi-1DAl	26.67	1.867	1.762[b]	59.24	16.3/15.9/17.0

[a]The nominal Si:Al ratio is 16 (64, 32, 8); the theoretical value presented in the table is the value calculated from the precise masses of reactants introduced during the synthesis (n_{Si}, n_{RSi}, n_M, n_{DIPE}).[b]0.214 mmol $AlCl_3$ added at the beginning of the reaction, 1.548 mmol 8 hrs later (autoclave cooled down, put back into the glovebox, opened, the rest of $AlCl_3$ added into the reaction mixture, the autoclave was then re-sealed and kept in an oven at 110 °C for remaining 64 hrs for gelation.

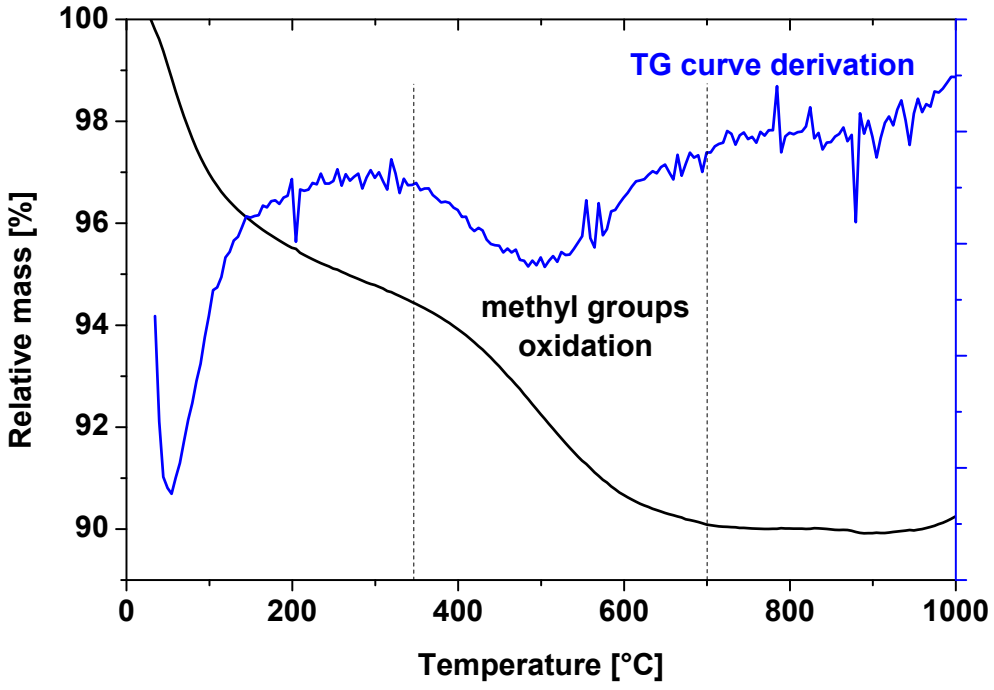

Fig. 1S: TG analysis of sample 15Si-1MeSi-1Al.

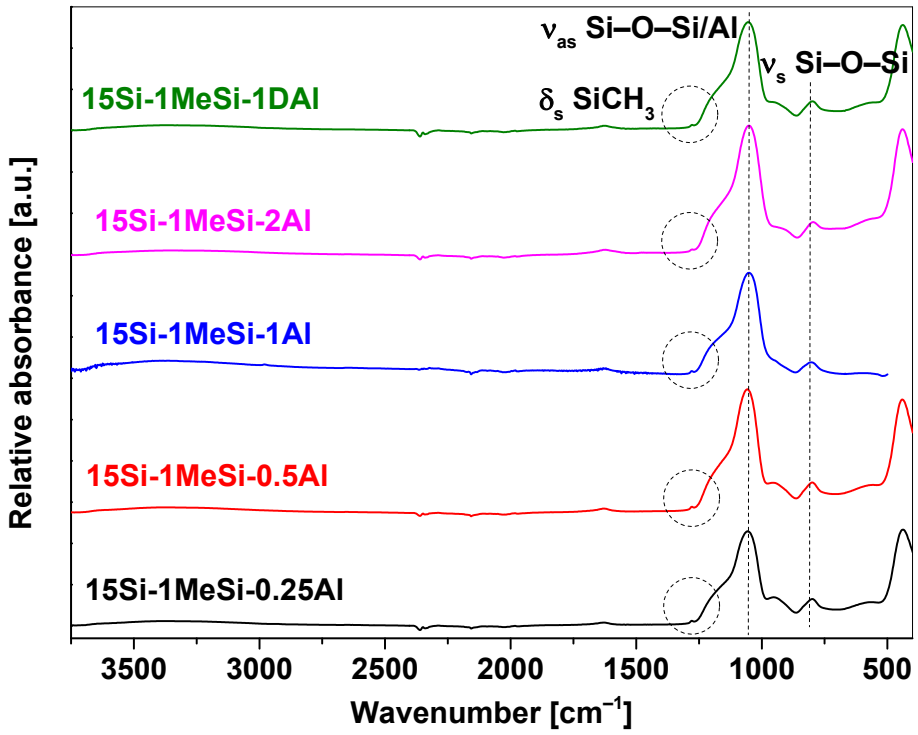

Fig. 2S: IR spectra of NHSG prepared samples with different Si/Al ratio and delayed Al addition.

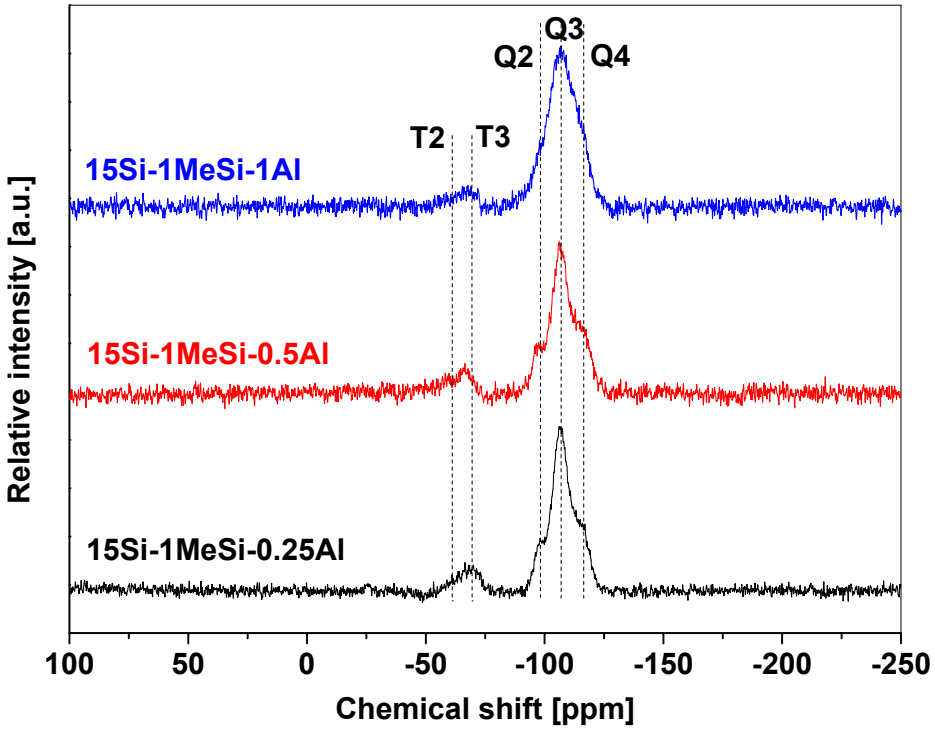

Fig. 3S: ^{29}Si CPMAS NMR spectra of NHSG prepared samples with different Si/Al loading.

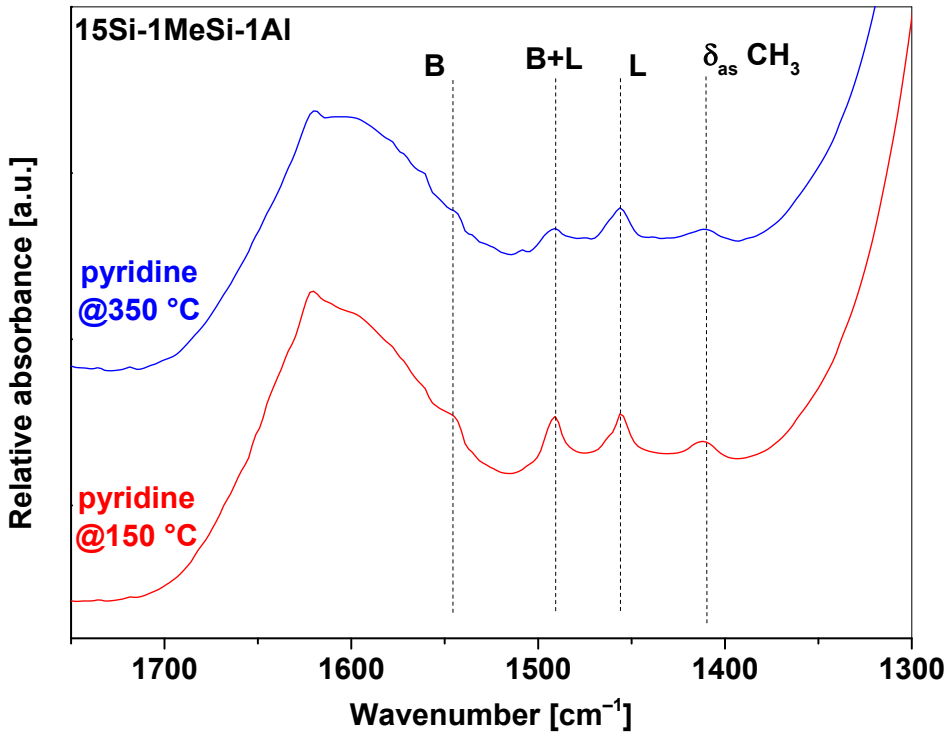

Fig. 4S: IR spectra of **15Si-1MeSi-1Al**, after pyridine adsorption and degassed at different temperatures.

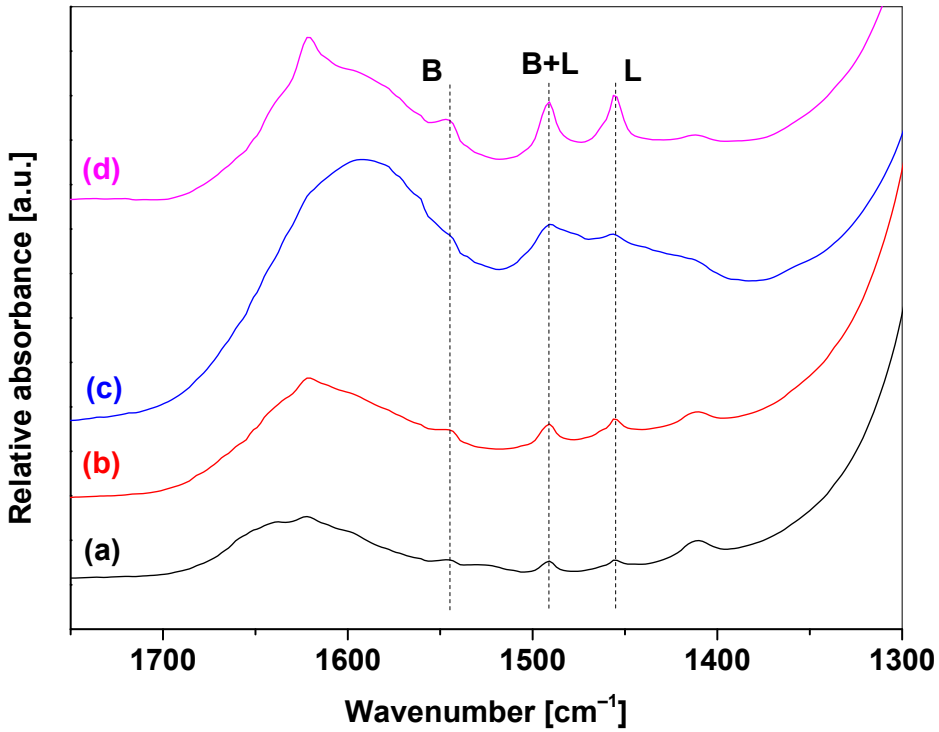

Fig. 5S: IR spectra of **15Si-1MeSi-0.25Al** (a), **15Si-1MeSi-0.5Al** (b), **15Si-1MeSi-2Al** (c), and **15Si-1MeSi-1DAl** (d) after evacuation at 350 °C, pyridine adsorption, and degassed at 150 °C.

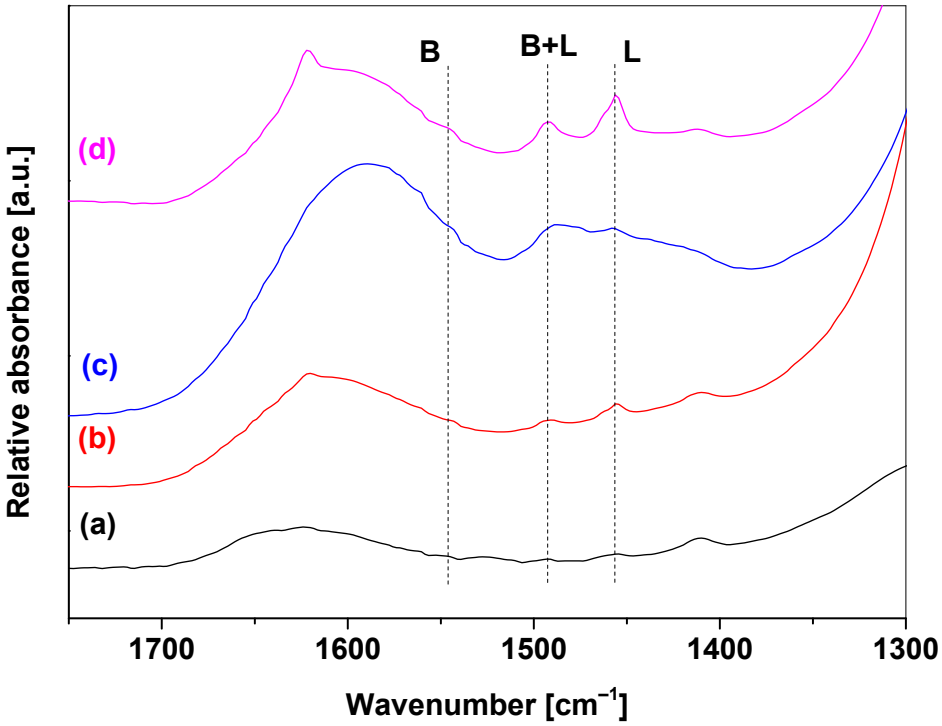

Fig. 6S: IR spectra of **15Si-1MeSi-0.25Al** (a), **15Si-1MeSi-0.5Al** (b), **15Si-1MeSi-2Al** (c), and **15Si-1MeSi-1DAl** (d) after evacuation at 350 °C, pyridine adsorption, and degassed at 350 °C.

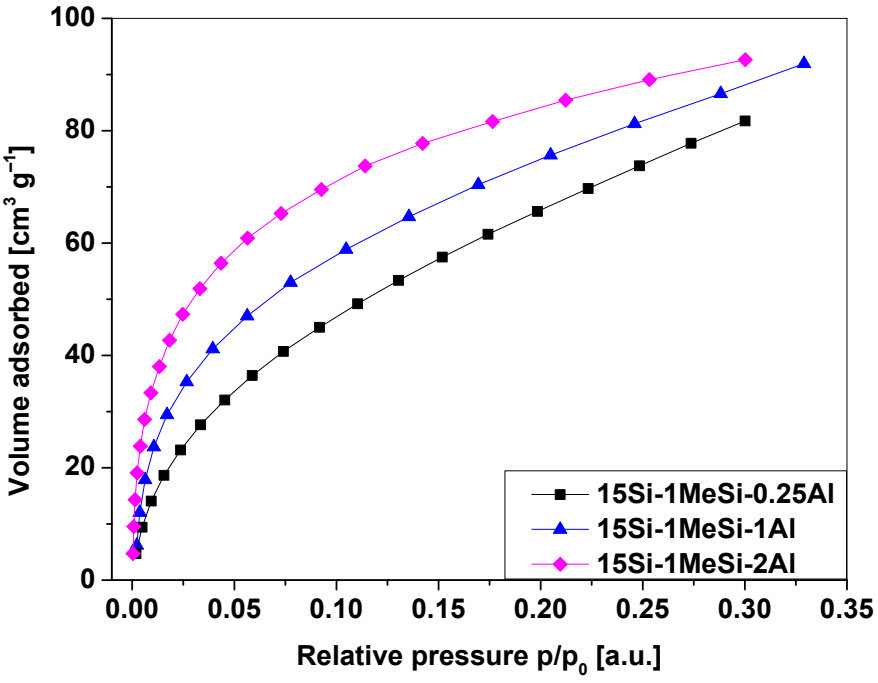

Fig. 7S: Water adsorption measurements performed at low p/p_0 (< 0.3) on samples with different Si:Al ratio.

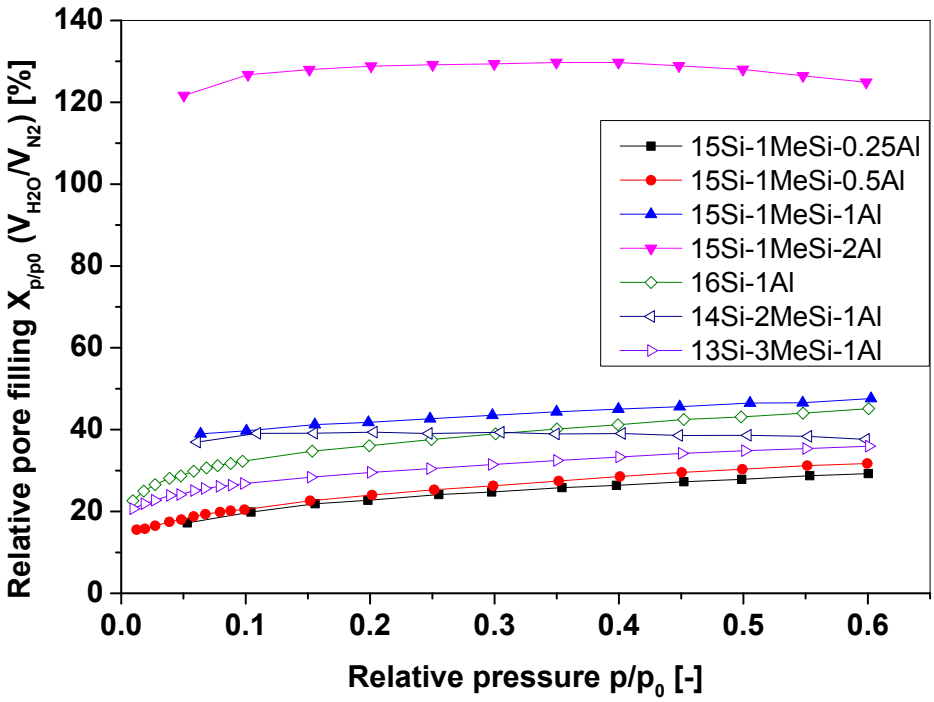

Fig. 8S: Volume of adsorbed H_2O over the volume of adsorbed N_2 at given p/p_0 values ($X_{p/p0}$; both adsorbates being considered as in liquid phase).

15Si-1MeSi-0.25Al (WCA = 25.3±2.4 °)

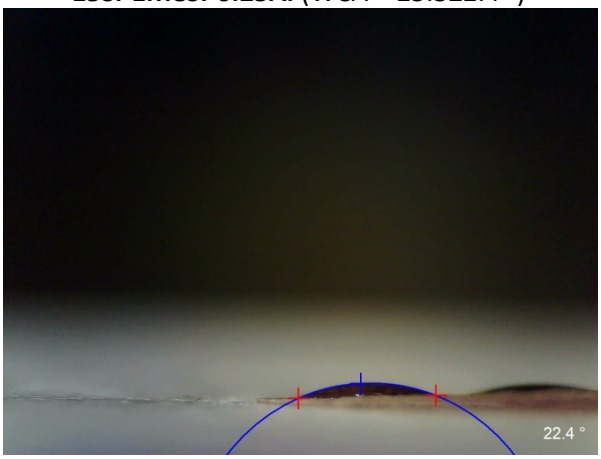

15Si-1MeSi-0.5Al (WCA = 20.1±1.7)

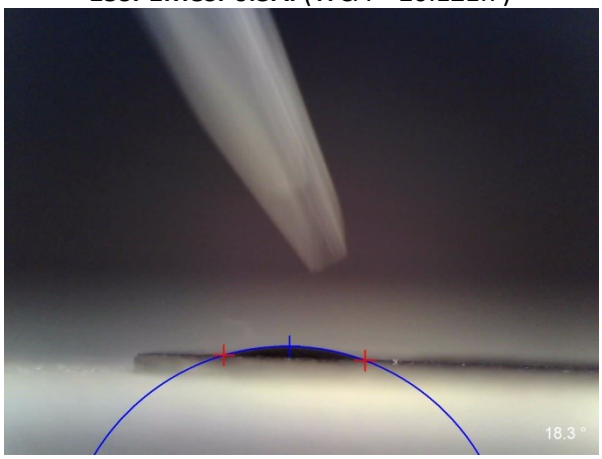

15Si-1MeSi-1Al (WCA = 26.7±1.6)

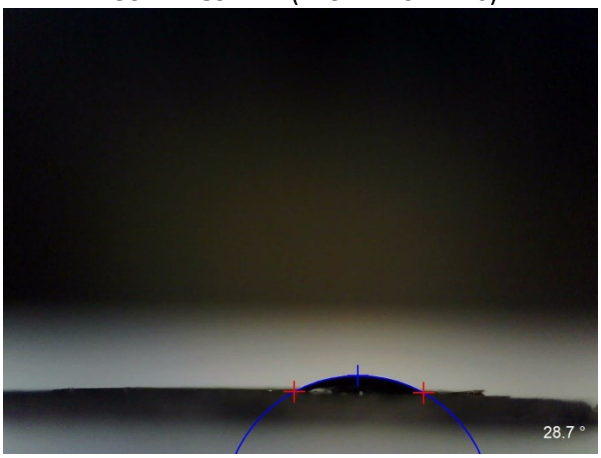

15Si-1MeSi-2Al (WCA = 20.0±2.0)

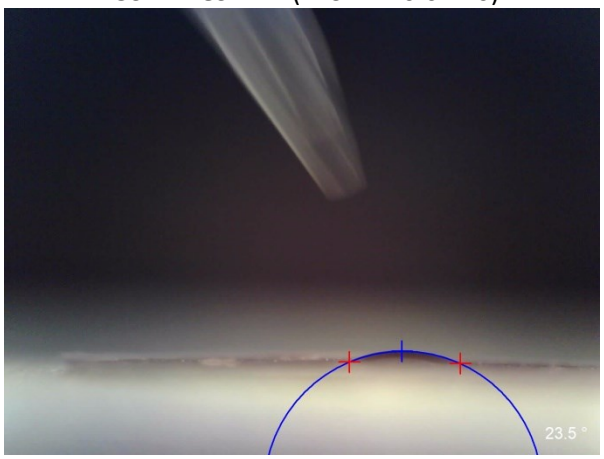

Fig. 9S: The results of water contact angle measurements for aluminosilicate samples with varying Si:Al ratio. Average numbers based on 5-10 measurements and the best captured image for each sample.

Table 2S: Ethanol conversion, yield and selectivity for ethylene and diethylether.

Sample	Temperature [°C]	Ethanol conversion [%]	Ethylene		Diethylether	
			Selectivity [%]	Yield [%]	Selectivity [%]	Yield [%]
15Si-1MeSi-0.25Al	205	17.8	54.3	9.7	27.8	4.9
	240	54.7	78.7	43.0	16.6	9.1
	275	94.4	88.3	88.4	5.0	4.8
15Si-1MeSi-0.5Al	205	25.8	70.0	18.1	41.0	10.6
	240	73.7	79.6	58.7	17.3	12.7
	275	98.5	95.6	94.1	2.6	2.5
15Si-1MeSi-1Al	205	36.1	66.7	23.9	50.0	18.1
	240	87.6	82.7	72.5	15.1	13.2
	275	100	97.4	97.4	0.4	0.4
15Si-1MeSi-2Al	205	16.8	59.8	10.1	46.3	7.8
	240	49.8	71.0	35.4	21.7	10.8
	275	78.7	88.8	69.9	8.6	6.8
15Si-1MeSi-1DAl	205	63.1	59.3	37.4	49.5	31.3
	240	98.7	97.4	96.1	2.6	2.6
	275	100	96.3	96.3	0	0
SACS commercial	215	24.6	8.4	2.1	115	28.3
	245	58.7	19.8	11.6	88.7	52.1
	275	80.8	43.7	35.3	57.0	46.1
HZSM-5 commercial	205	81.7	32.4	26.4	77.6	63.4
	240	99.8	97.9	97.8	0.6	0.6
	275	99.8	93.1	92.9	0.6	0.6
16Si-1Al	205	33.1	47.4	15.7	50.6	16.7
	240	81.8	72.9	59.6	22.7	18.5
	275	100	98.0	98.0	1.8	1.8
14Si-2MeSi-1Al	205	35.0	68.1	23.8	42.7	14.9
	240	90.9	84.5	76.8	14.0	12.7
	275	100	96.8	96.8	0.7	0.7
13Si-3MeSi-1Al	205	33.6	72.9	24.5	40.7	13.7
	240	88.6	84.6	75.0	15.6	13.8
	275	100	97.9	97.9	1.3	1.3

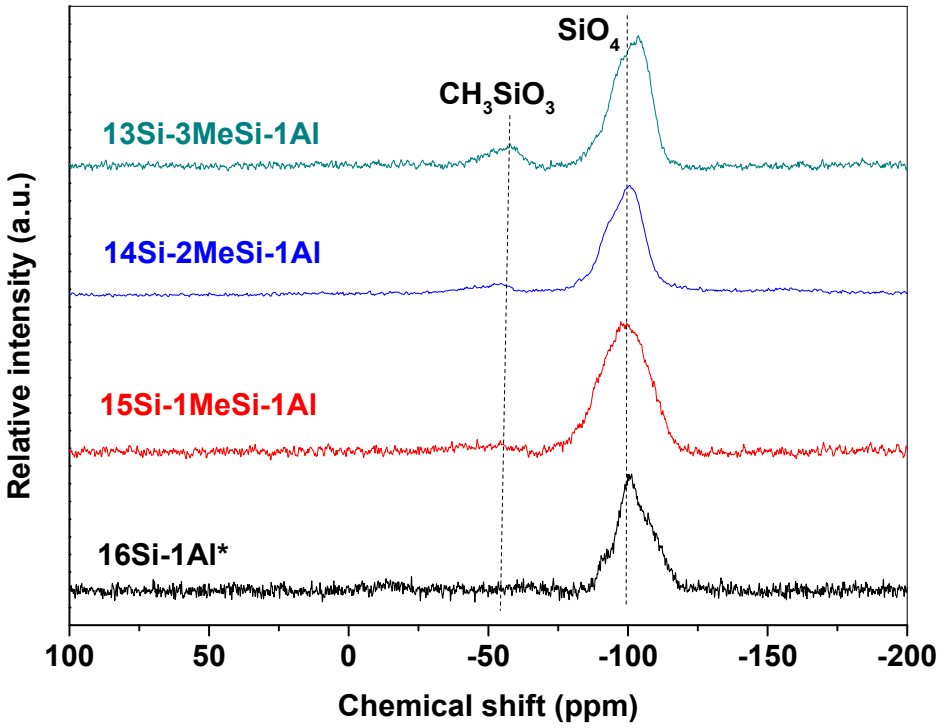

Fig. 10S: ^{29}Si MAS NMR spectra of NHSG prepared samples with different Si—CH_3 groups loading. Asterisk denotes ^{29}Si CPMAS NMR spectrum.

Table 3S: Experimental and nominal content of MeSi groups (at% based on Si molar amount)

Sample	Experimental[a] MeSi content [at%][b]	Theor. MeSi content [at%][b]
16Si-1Al	0	0
15Si-1MeSi-1Al	3.3	6.02
14Si-2MeSi-1Al	6.9	12.4
13Si-3MeSi-1Al	10	18.8

[a]Experimental values obtained from ^{29}Si MAS NMR spectra (Fig. 10S) by deconvolution and integration; [b]Percentage of MeSi groups out of all Si species in the reaction mixture (n($MeSiCl_3$) + n($SiCl_4$))

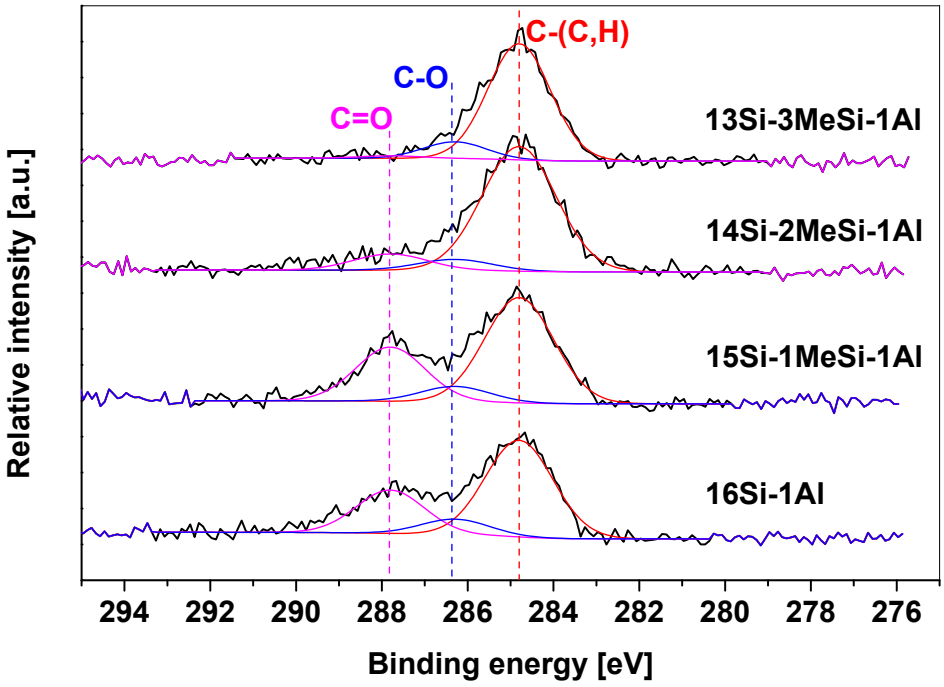

Fig. 11S: XPS spectra (C 1s) of NHSG prepared aluminosilicates with various MeSi groups content.

Table 4S: Carbon contents in the surface layers of catalysts determined by XPS.

Sample	C content total (at%)	C-(C,H) content (at%)
16Si-1Al	4.74	2.94
15Si-1MeSi-1Al	5.92	3.56
14Si-2MeSi-1Al	6.41	5.26
13Si-3MeSi-1Al	8.55	7.35

Table 5S: Average areas of peaks attributed to CH_2^+, CH_3^+, $SiCH_2^+$, $SiCH_3^+$, $AlSiO_3^-$, and $AlSi_2O_5^-$ ions found at m/z = 14.015, 15.023, 41.986, 42.992, 102.94, and 162.92, respectively, in mass spectra obtained via ToF-SIMS analyses.

Sample	CH_2^+ peak area	CH_3^+ peak area	$SiCH_2^+$ peak area	$SiCH_3^+$ peak area	$C_3H_7^+$ peak area	$AlSiO_3^-$ peak area	$AlSi_2O_5^-$ peak area
16Si-1Al	4185	22677	5311	18044	13680	603	318
15Si-1MeSi-1Al	5375	26006	6176	15466	15738	510	252
13Si-3MeSi-1Al	5538	23373	9674	26244	14017	698	406

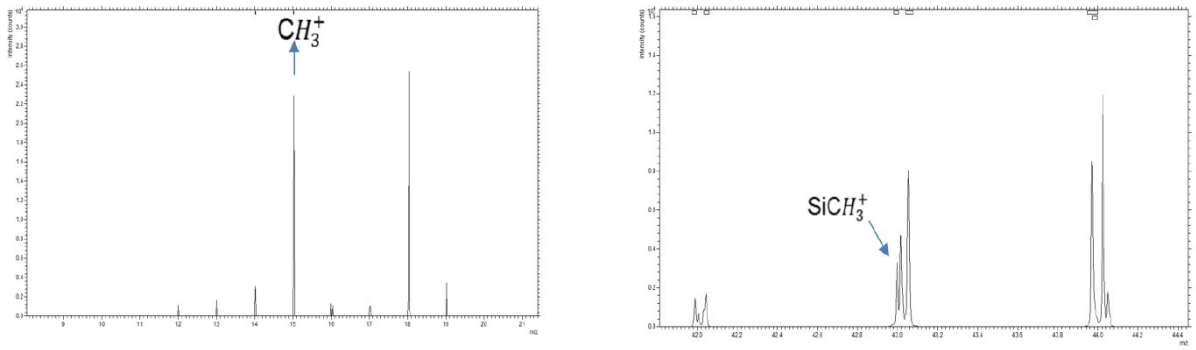

Fig. 12S: Relevant parts of mass spectra used for Si—CH_3 groups analysis in surface layer by ToF-SIMS.

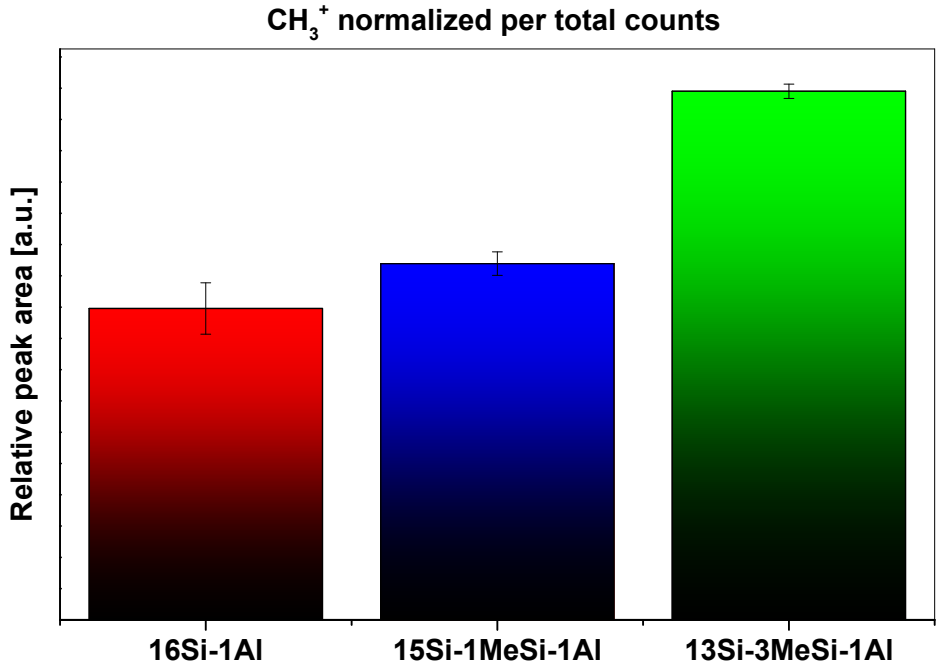

Fig. 13S: Comparison of samples with different Si—CH_3 groups loading in terms of relative peak areas of masses corresponding to CH_3^+ ions in mass spectra obtained by ToF-SIMS.

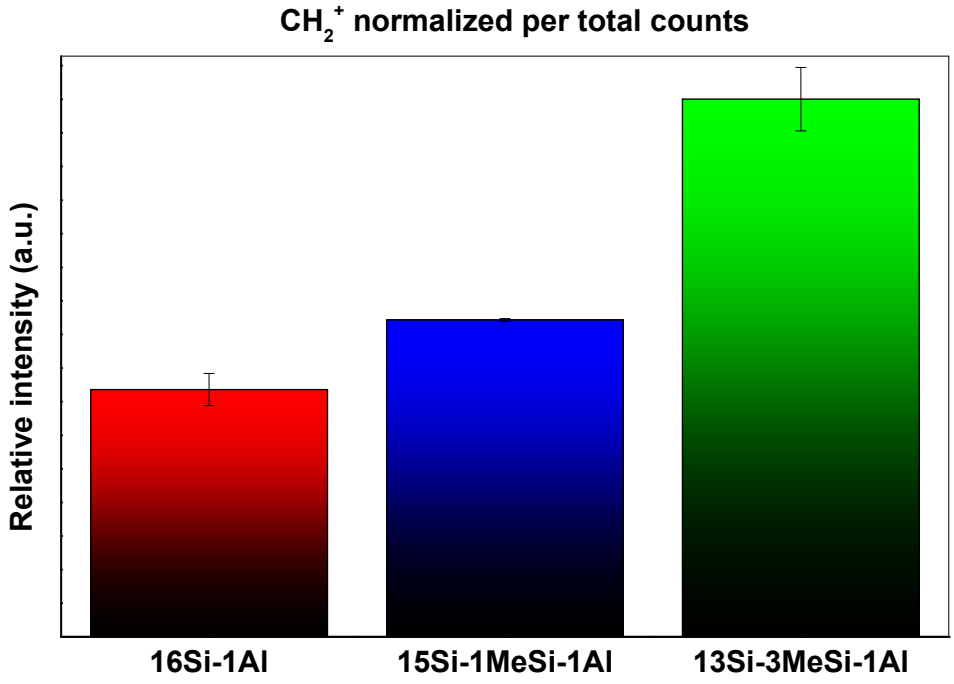

Fig. 14S: Comparison of samples with different Si—CH_3 groups loading in terms of relative peak areas of masses corresponding to CH_2^+ ions in mass spectra obtained by ToF-SIMS.

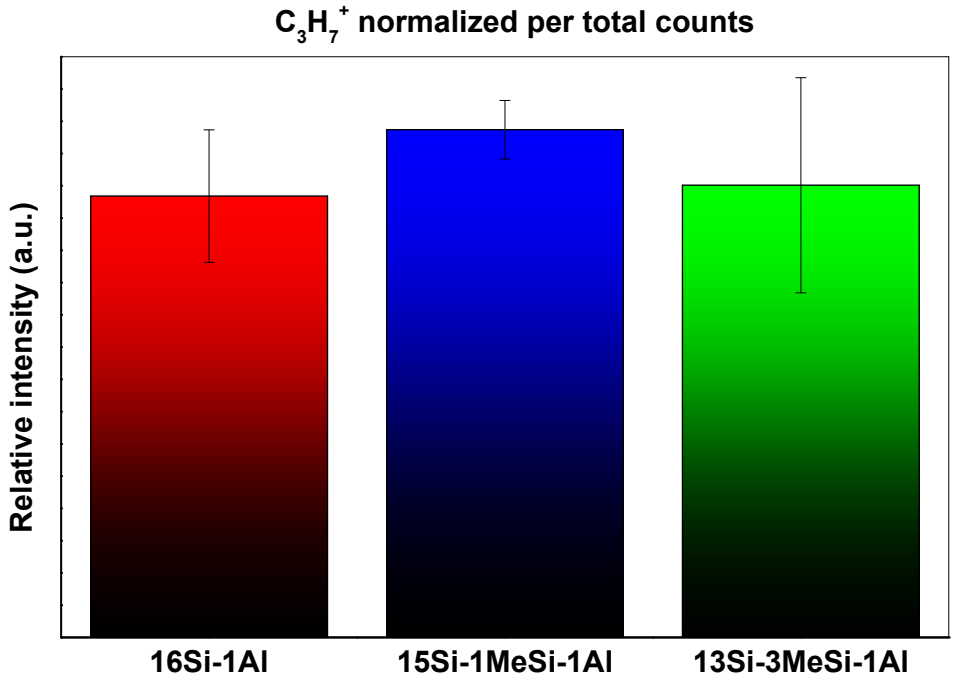

Fig. 15S: Comparison of samples with different Si—CH_3 groups loading in terms of relative peak areas of masses corresponding to $C_3H_7^+$ ions in mass spectra obtained by ToF-SIMS.

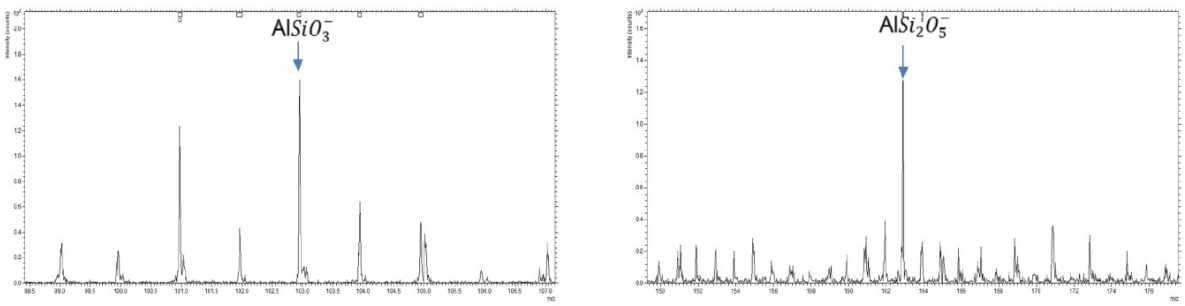

Fig. 16S: Relevant parts of mass spectra used for homogeneity analysis by ToF-SIMS.

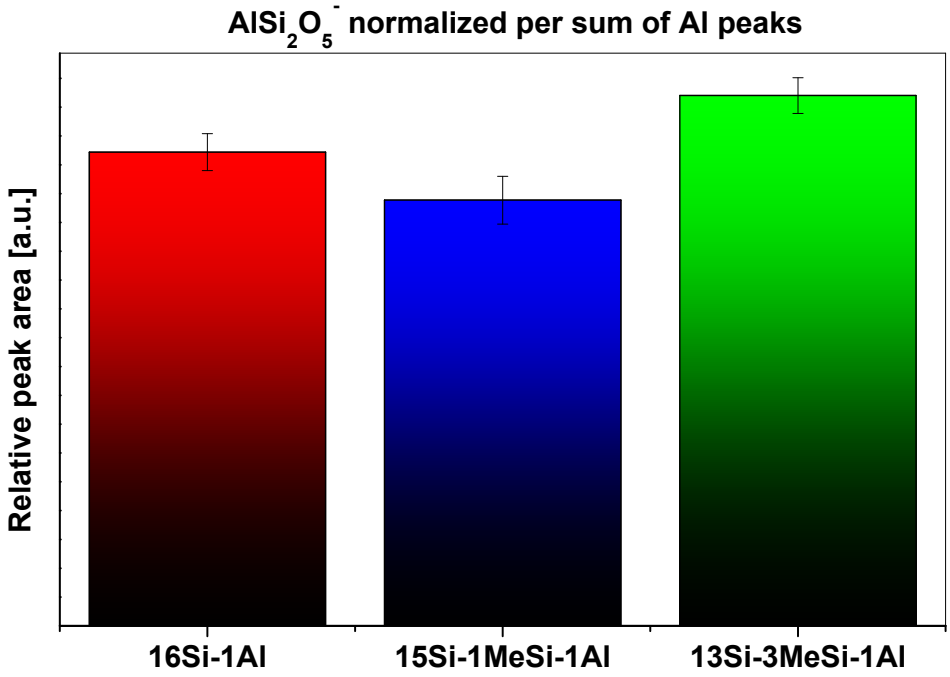

Fig. 17S: Comparison of samples with different Si—CH_3 groups loading in terms of relative peak areas of masses corresponding to $AlSi_2O_5^-$ ions (mixed Al-Si clusters) in mass spectra obtained by ToF-SIMS.

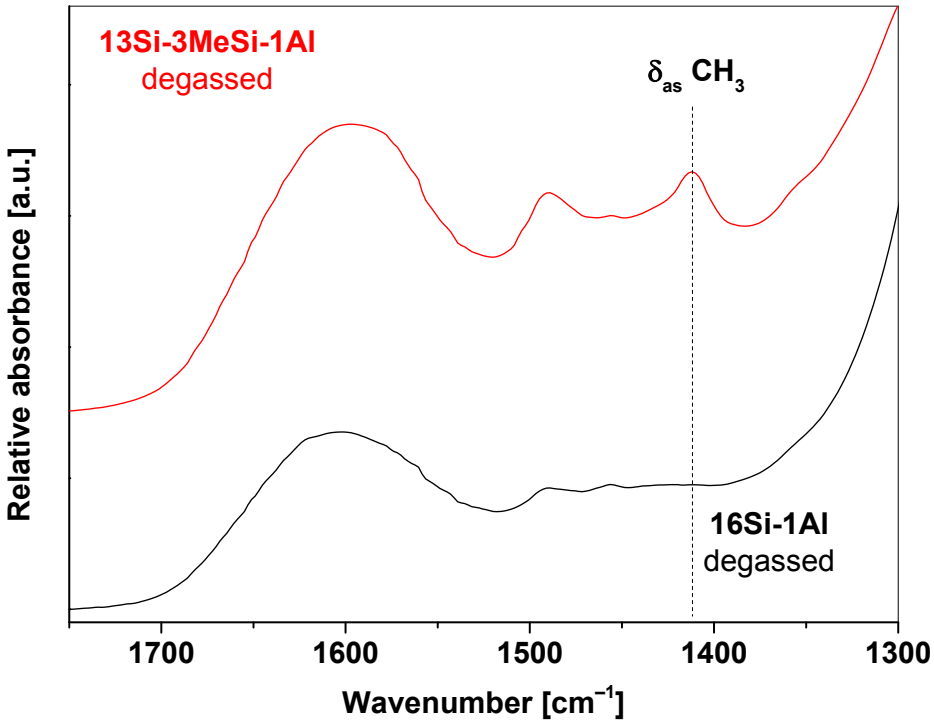

Fig. 18S: IR spectra of **16Si-1Al** and **13Si-3MeSi-1Al** after evacuation at 350 °C.

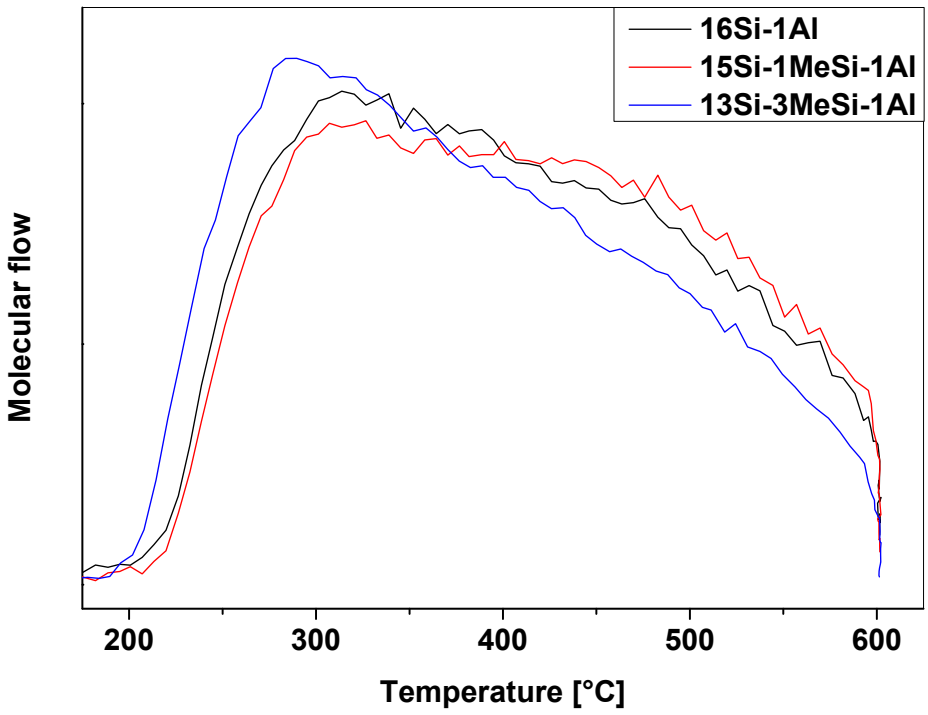

Fig. 19S: NH_3-TPD curves of samples with different Si—CH_3 groups loading showing only subtle changes during methylation of NHSG prepared aluminosilicates.

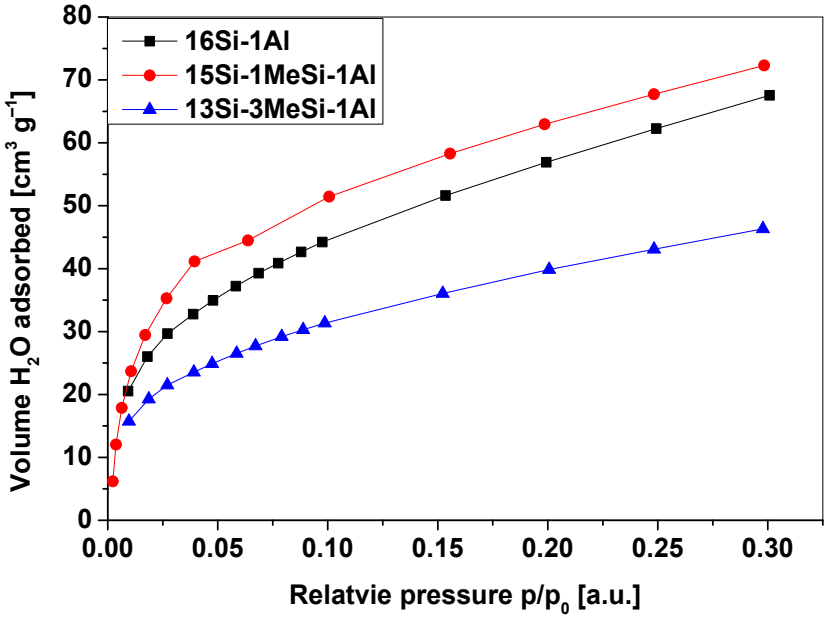

Fig. 20S: Water adsorption measurements performed at low p/p_0 (< 0.3) on samples with different MeSi groups loading.

16Si-1Al (WCA = 21.5±1.7 °)

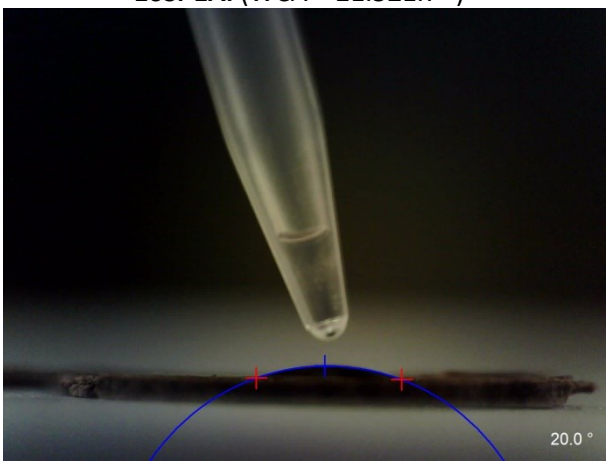

15Si-1MeSi-1Al (WCA = 26.7±1.6)

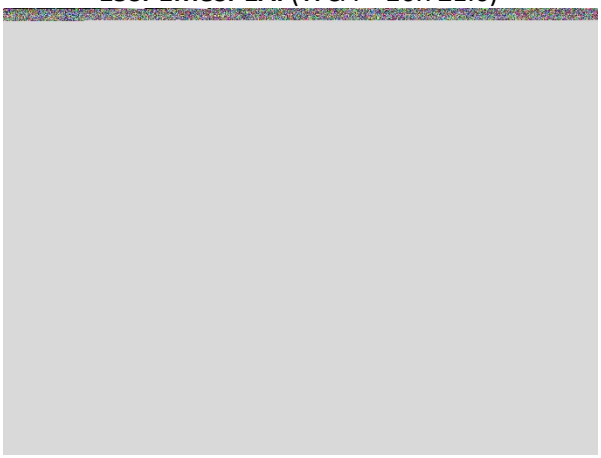

14Si-2MeSi-1Al (WCA = 31.7±2.5)

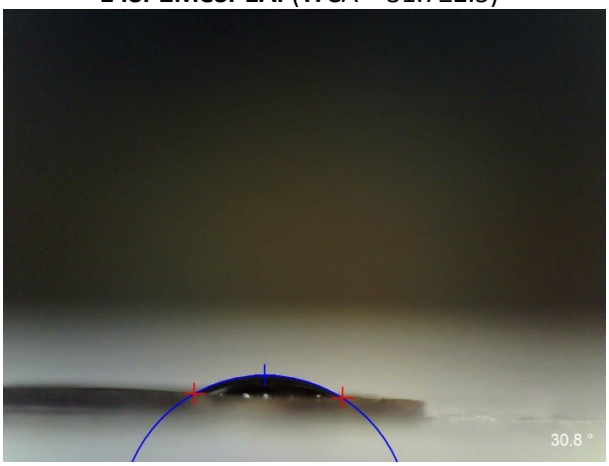

13Si-3MeSi-1Al (WCA = 31.8±2.7)

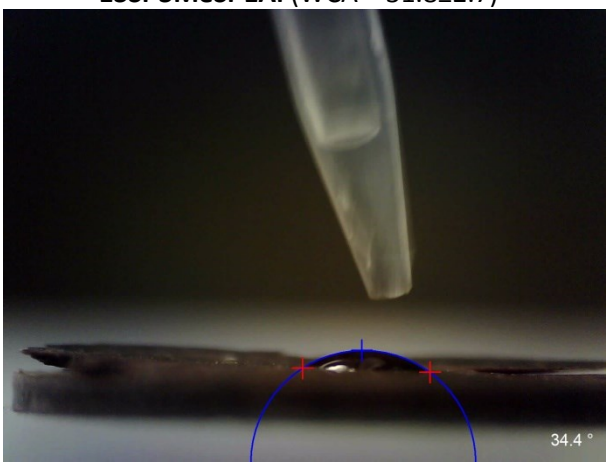

Fig. 21S: The results of water contact angle measurements for aluminosilicate samples with varying CH_3Si groups content. Average numbers based on 5-10 measurements and the best captured image for each sample.

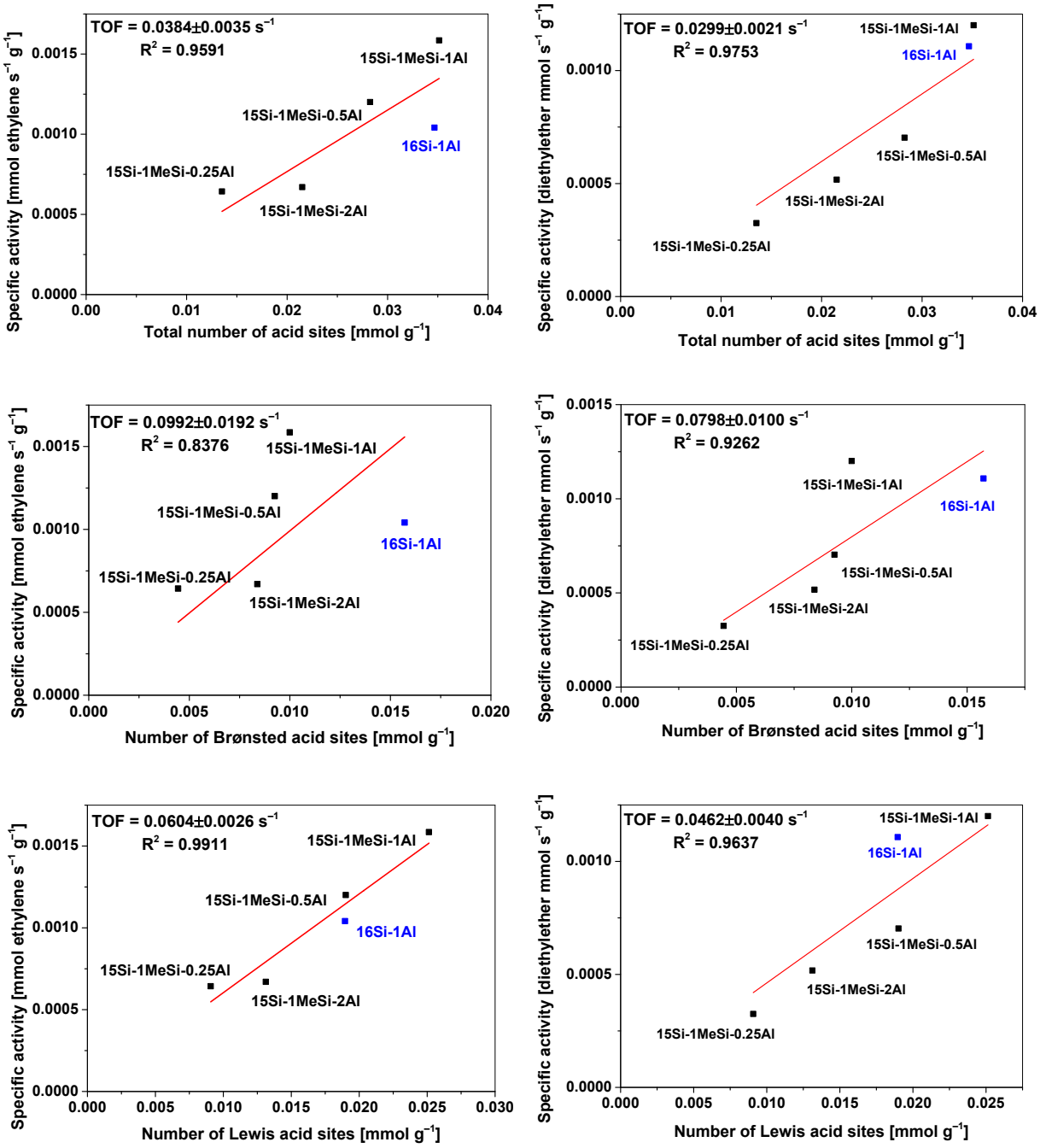

Fig. 22S: Plots of the specific activity (expressed in mmol of ethylene or diethylether produced by g of catalyst per s at 205 °C) vs. amount of acid sites based on the IR-pyridine analyses (total, Lewis, and Brønsted). Plots decribing ethylene are on the left side, plots describing diethylether are on the right side. The slope of the linear fit is a turnover frequency of ethanol dehydration to ethylene/diethylether expressed in mmol of ethylene produced per second and per mmol of total/Lewis/Brønsted sites. The best fit for ethylene was observed for the number of Lewis acid sites (left), the best fit for diethylether was observed for the total number of acid sites.

Table 6S: Comparison of fresh and spent NHSG aluminosilicate catalysts in terms of their mass loss during TGA, porosity, and catalytic performance.

Sample	Mass loss [%]		SA_{BET} rel. drop [%]	V_{total} rel. drop [%]	Conversion drop [%]	Ethylene sel. drop [%]
	fresh	spent				
16Si-1Al	12.4	11.8	9.5	13.8	25.2	7.3
15Si-1MeSi-1Al	9.7	11.4	9.0	15.3	24.1	9.0
13Si-3MeSi-1Al	11.5	11.3	23.2	17.4	26.9	13.6
15Si-1MeSi-0.5Al	-	-	28.3	39.0	18.7	6.7

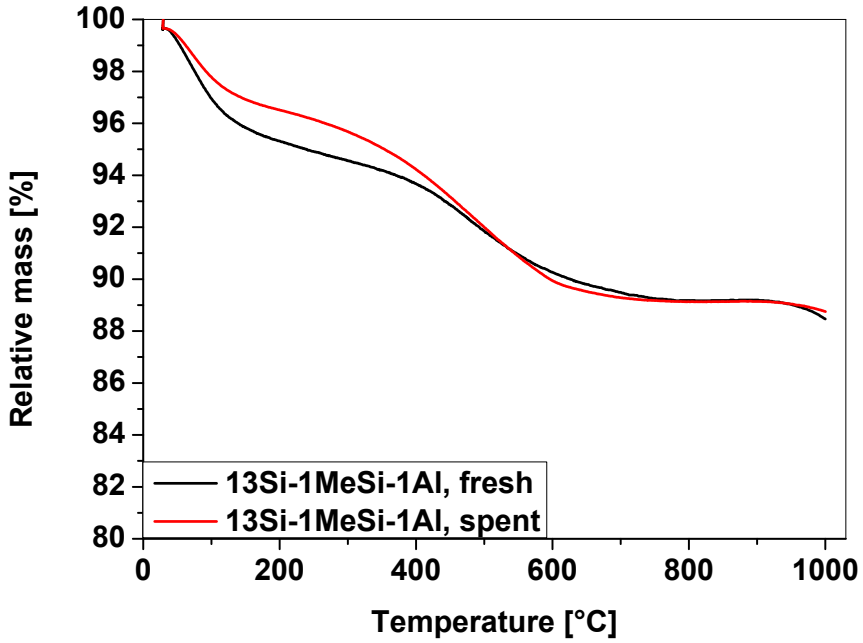

Fig. 23S: Comparison of TG analyses of spent and fresh 13Si-3Mesi-1Al catalyst.

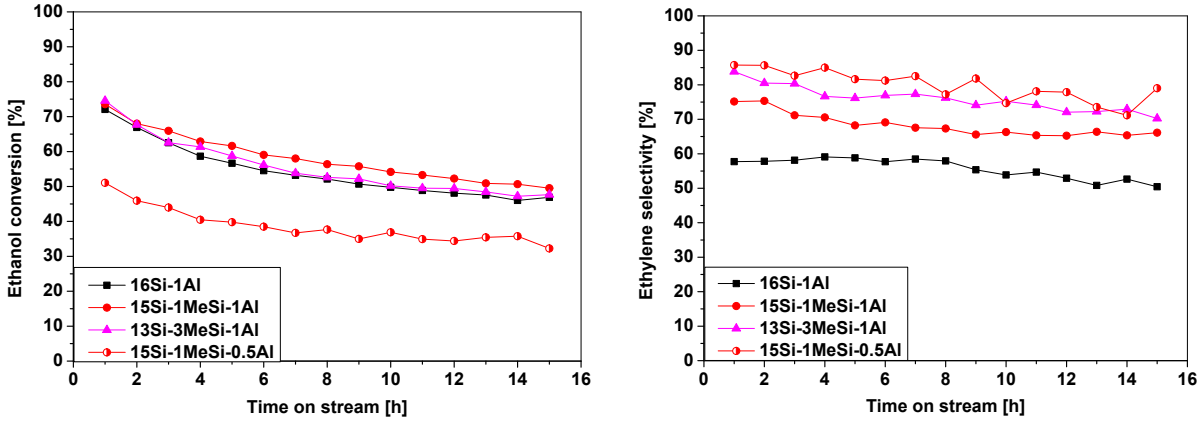

Fig. 24S: Conversion (left) and ethylene selectivity (right) at 240 °C over NHSG aluminosilicate catalysts during 15 h time on stream stability test.

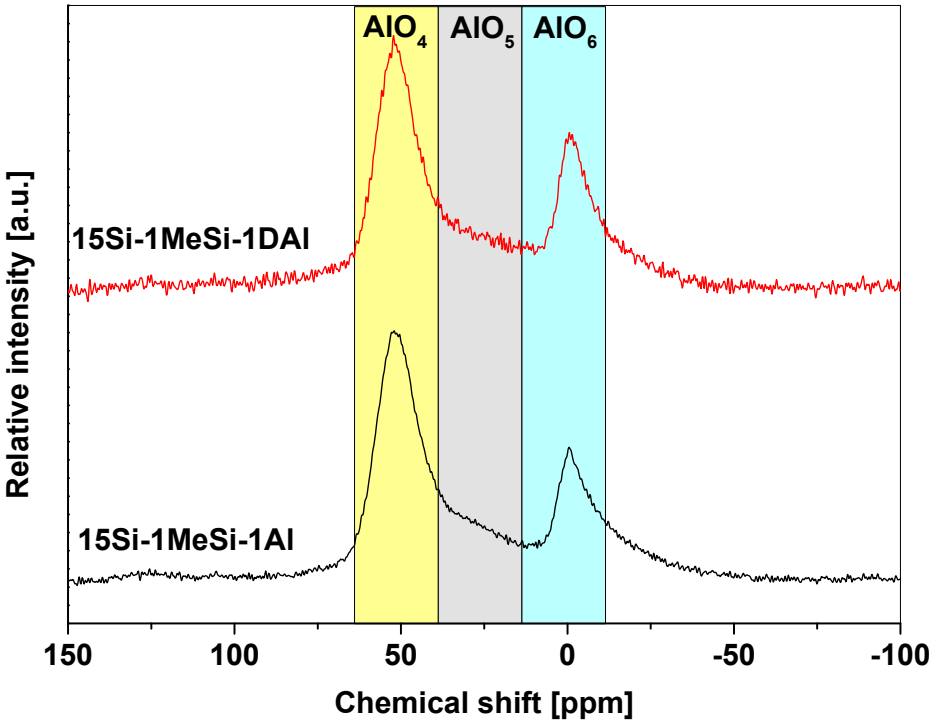

Fig. 25S: Comparison of ^{27}Al MAS NMR spectra of **15Si-1MeSi-1Al** and **15Si-1MeSi-1DAl**.